Applied Surface Science 263 (2012) 440–444

Applied Surface Science

journal homepage: www.elsevier.com/locate/apsusc

Chemically deposited In_2S_3–Ag_2S layers to obtain $AgInS_2$ thin films by thermal annealing

S. Lugo [a], Y. Peña [a,*], M. Calixto-Rodriguez [b], C. López-Mata [c], M.L. Ramón [b], I. Gómez [a], A. Acosta [a]

[a] Universidad Autónoma de Nuevo León, UANL, Fac. de Ciencias Químicas, Av. Universidad S/N Ciudad Universitaria San Nicolás de Los Garza Nuevo León, C.P. 66451 Mexico
[b] Centro de Investigación en Energía-Universidad Nacional Autónoma de México, 62580, Temixco, Morelos, Mexico
[c] Instituto Tecnológico de Chetumal, Av. Insurgentes No. 330, C.P. 77013, Col. David Gustavo Gtz., Chetumal, Quintana Roo, Mexico

ARTICLE INFO

Article history:
Received 9 February 2012
Received in revised form 1 September 2012
Accepted 16 September 2012
Available online 24 September 2012

Keywords:
Silver indium sulfide
Thin films
Chemical bath deposition

ABSTRACT

$AgInS_2$ thin films were obtained by the annealing of chemical bath deposited In_2S_3–Ag_2S layers at 400 °C in N_2 for 1 h. According to the XRD and EDX results the chalcopyrite structure of $AgInS_2$ has been obtained. These films have an optical band gap, E_g, of 1.86 eV and an electrical conductivity value of 1.2×10^{-3} $(\Omega\,cm)^{-1}$.

1. Introduction

The $AgInS_2$ compound can be grown as tetragonal and orthorhombic phase [1]. In the tetragonal crystal structure it shows two direct band gaps, at 1.86 and 2.02 eV [1], while in the orthorhombic crystal structure it shows two band gaps at 1.96 and 2.04 eV [2]. $AgInS_2$ belongs to the I-III-VI_2 group. It is one of the least studied materials compared to the thorough investigated copper indium chalcogenides (CIS) used in photovoltaic device applications [2,3]. For example, making a comparison between $CuInS_2$ and $AgInS_2$ we have found out that $CuInS_2$ has an optical band gap of 1.5 eV while $AgInS_2$ has a wider band gap (1.86–2.04 eV); both materials have a high absorption coefficient; $CuInS_2$ shows a p-type electrical conductivity, and although $AgInS_2$ shows a n-type electrical conductivity [4], it can be doped with Sb [5] and Sn [6] atoms to change its conductivity to p-type.

Several methods such as thermal evaporation [7], spray pyrolysis [8], co-evaporation [9], and chemical bath deposition (CBD) [10] have been used to obtain $AgInS_2$ thin films, but CBD has proved to be the most attractive, easy to apply, less expensive and suitable for large area deposition. Moreover, in comparison with thermal evaporation and co-evaporation methods CBD does not require high vacuum systems.

In this work, the results of the structural, chemical composition, optical and electrical characterization of the polycrystalline silver indium sulfide thin films obtained through the annealing of chemically deposited In_2S_3–Ag_2S layers are presented.

2. Experimental details

2.1. Deposition of In_2S_3 thin films

In_2S_3 thin films were deposited by chemical bath deposition method using a mixture of the following reagents in the order described here: 10 mL of $In(NO_3)_3$ 0.1 M, 2 mL of CH_3COOH 0.1 M, 16 mL of CH_3CSNH_2 1 M, and water to complete a volume of 100 mL. The glass substrates (Corning, 25 mm × 75 mm) were placed vertically in the solution. The chemical deposition was carried out at 35 °C for 22 h, since lower deposition temperature produces thinner films, and higher deposition temperature accelerates the precipitation of the solution resulting in films of low quality.

2.2. Deposition of Ag_2S thin films

Chemically deposited silver sulfide thin films were obtained by following the procedure given in Ref. [11] using: 12.5 mL of 0.1 M solution of $AgNO_3$, 4.5 mL of 1 M solution of $Na_2S_2O_3$, 5 mL of 0.5 M solution of $C_3H_8N_2S$ in the given sequence then adding deionized water while stirring the solution until completing a 100 mL volume. Indium sulfide thin films prepared previously were used as

* Corresponding author. Tel.: +52 8183294000x6363/8183294010; fax: +52 8183765375.
E-mail address: yolapm@gmail.com (Y. Peña).

0169-4332/$ – see front matter © 2012 Elsevier B.V. All rights reserved.
http://dx.doi.org/10.1016/j.apsusc.2012.09.077

substrates. The substrates were placed vertically in the solution at 35 °C for 1, 2 or 3 h. For this study we chose a deposition time of 1 h.

2.3. Thermal annealing

The thin films of In_2S_3–Ag_2S were thermally annealed in a tubular furnace (Thermolyne 21100). We have made some annealing experiments of the In_2S_3/Ag_2S layers at 350 °C for 60 min and at 400 °C for 60 and 90 min in N_2 atmosphere. For this study we chose an annealing temperature and time of 400 °C and 60 min in order for it to react and convert the In_2S_3–Ag_2S films into $AgInS_2$.

2.4. Characterization

X-ray diffraction (XRD) patterns were recorded on a Rigaku D-Max 2000 diffractometer using Cu Kα radiation (λ = 1.5406 Å). The chemical composition of the annealed films was determined by energy dispersive X-ray spectroscopy (EDX) using an Inca Oxford Instruments system attached to the scanning electron microscope. The surface morphology was studied by scanning electron microscopy (SEM) JEOL model JSM 5800LV at 1 kV and 25,000×. Field emission atomic force microscopy (FE-AFM) analysis was done using a JEOL JSM-6701 F equipment, the thickness of the film was measured by AFM and SEM. The optical transmittance at normal incidence, $T(\lambda)$, and specular reflectance spectra, $R(\lambda)$, of the films were measured with a spectrophotometer Shimadzu model UV-1800 in the UV–vis-NIR region (190–1100 nm wavelength range). Hall measurements were recorded to obtain the value and type of the electrical conductivity. The temperature dependent conductivity measurements were performed using equipment named Janis CCS 400/202 N with a temperature range of 300–10 K, and in order to do this it was necessary to apply a pair of coplanar carbon paint electrodes.

3. Results and discussion

3.1. Structural characterization and chemical compositional analysis

The $AgInS_2$ films were obtained by the deposition in sequence of layers of Ag_2S, deposited at 35 °C for 1 h, over an In_2S_3 film previously deposited at 35 °C for 22 h. When we performed the annealing of the structure In_2S_3/Ag_2S using a Ag_2S layer deposited for 2 or 3 h, the XRD results showed that the film has a mixture of phases: $AgInS_2$ (tetragonal and orthorhombic) and Ag_2S (acanthite).

When we made the annealing experiments of the In_2S_3/Ag_2S layers at 400 °C for 60 and 90 min we found from the XRD results that there is no difference between the annealing time considered at 60 and 90 min. When we performed the annealing of the In_2S_3/Ag_2S layers at 350 °C, we found out a mixture of phases (In_2S_3 and $AgInS_2$), not just the one which corresponds to the $AgInS_2$. In addition, the XRD results showed that $AgInS_2$ film has not crystallized completely at 350 °C. So, this was the reason, we decided to perform the annealing of the structure In_2S_3/Ag_2S at 400 °C for 1 h.

The chemical reactions for the formation of $AgInS_2$ are described below:

The presence of the air in the solution environment favoured the production of oxide at a lower deposition temperature (35 °C). There are two possibilities proposed to explain the formation of In_2O_3 from the thioacetamide–In(III) solution. On one hand, the precipitation of the hydroxide [12]:

$$In^{3+} + 3H_2O \rightarrow In(OH)_3 + 3H^+ \quad (1)$$

$$2In(OH)_3 \rightarrow In_2O_3 + 3H_2O \quad (2)$$

A second route can be proposed for the deposition of thin films of In(O;OH)S, thioacetamide was used as source of S^{2-} through the hydrolysis in an acidic environment; and acetic acid (AcOH) was used as complexing agent; the entire reaction can be written as follows [13]:

$$[In(Ac)_{4-x}] + CH_3SCNH_2 \rightarrow [In(O;OH)S]_{film} + (4-x)HAc + NCNH_2 + H_2O \quad (3)$$

The chemical reactions for the deposition of Ag_2S films taking place in the chemical bath could be considered as below. Silver ions, Ag^+, in the bath combine with $S_2O_3{}^{2-}$ to initially form an insoluble $Ag_2S_2O_3$, which in excess of $S_2O_3{}^{2-}$, form soluble complexes:

$$[Ag_2(S_2O_3)_3]^{4-} \rightarrow 2Ag^+ + 3(S_2O_3)^{2-} \quad (4)$$

$$Ag_2S_2O_3 + H_2O \Leftrightarrow Ag_2S + SO_4{}^{2-} + 2H^+ \quad (5)$$

The overall reaction of the ternary system films containing the $AgInS_2$ phase is given by:

$$[In(O;OH)S]_{film} + Ag_2S_{film\,400\,^\circ C} \rightarrow 2Ag^+ + 2In^{3+} + 2S^{2-} \quad (6)$$

$$2Ag^+ + 2In^{3+} + 2S^{2-} \rightarrow 2AgInS_{2\,film}$$

or

$$In_2S_{3\,film} + Ag_2S_{film} \rightarrow 2Ag^+ + 2In^{3+} + 2S^{2-} \quad (7)$$

$$2Ag^+ + 2In^{3+} + 2S^{2-}{}_{400\,^\circ C} \rightarrow 2AgInS_{2\,film}$$

From the XRD pattern of the sample it was found that the ternary system contains the $AgInS_2$ phase (see Fig. 1), which is in agreement with literature [14]. The XRD pattern shown in Fig. 1 corresponds to both structures of $AgInS_2$: the tetragonal (chalcopyrite) structure of $AgInS_2$ T(JCPDS 25-1330) with reflections in (1 1 2), (2 0 0), (2 2 0), (2 0 4), and (3 1 2); and the orthorhombic structure of $AgInS_2$ O(JCPDS 25-1328) with reflections in (2 0 0), (0 0 2), (1 2 1), (0 4 0), (3 2 0), and (0 4 2). Additionally, Fig. 1 shows two peaks (2 2 2) and (6 2 2) which correspond to indium oxide (In_2O_3).

From the chemical compositional analysis we found the following results Ag = 22.21 at%, In = 29.52 at%, and S = 48.27 at%. The error margin in EDX data is 5%. These results showed that the composition of the film is close to the stoichiometric composition of $AgInS_2$.

3.2. SEM and AFM measurements

Fig. 2(a) shows a typical SEM image of the morphology of the In_2S_3–Ag_2S samples, measured after the films reacted thermally in N_2 at 400 °C for 1 h. In this picture we can see that there are clusters of quasi-spherical shape of varying sizes. Fig. 2(c) shows a cross sectional SEM image of the same In_2S_3–Ag_2S sample. In this picture we can see that the film thickness is in the order of 200 nm.

Fig. 2(b) shows a typical AFM image of the surface topography in 3D of the In_2S_3–Ag_2S samples. This film shows that after the thermal annealing small grains had coalesced, resulting in bigger grains on the film surface. The average film thickness was 270 nm for the resulting $AgInS_2$ film.

3.3. Optical and electrical characterization

Optical transmission, $T(\lambda)$, and reflection spectra, $R(\lambda)$, were recorded in the range of 300–1100 nm. Fig. 3 shows $T(\lambda)$ and $R(\lambda)$ responses for $AgInS_2$ film. The absorption coefficient (α) was calculated using $T(\lambda)$ and $R(\lambda)$ data and the well known expression, for direct optical transitions [15,16], given by

$$\alpha h\nu = A(h\nu - E_g)^r \quad (1)$$

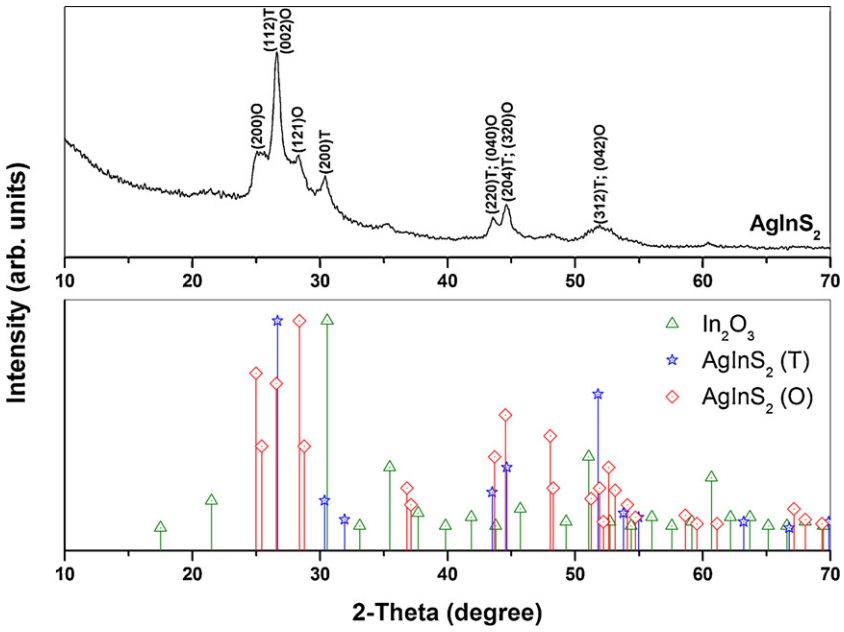

Fig. 1. X-ray diffraction pattern for $AgInS_2$ film (after annealing the In_2S_3–Ag_2S sample in N_2 at 400 °C for 1 h). "T" corresponds to the tetragonal (chalcopyrite) structure and "O" to the orthorhombic structure of the $AgInS_2$.

where A is a constant, and E_g is the optical band gap. In this equation $r = 1/2$ for direct allowed optical transitions and 3/2 for the direct forbidden ones. The band-gap value can be obtained from the best linear approximation in the $(\alpha h\nu)^{1/r}$ vs. $h\nu$ plot and its extrapolation to $(\alpha h\nu)^{1/r} = 0$. Fig. 4 shows the $(\alpha h\nu)^2$ vs. $h\nu$ plot for $AgInS_2$ film. The band gap value obtained was $E_g = 1.86$ eV, this value agrees with what was reported for chalcopyrite $AgInS_2$ ($E_g = 1.87$ eV) [17].

The value of the electrical conductivity for $AgInS_2$ thin film was $1.2 \times 10^{-3}\,(\Omega\,\mathrm{cm})^{-1}$. Hall measurements indicated that the $AgInS_2$ film has n-type electrical conductivity.

The temperature dependent conductivity measurements were carried out (see Fig. 5). The conductivity is given by Ref. [18]:

$$\sigma = \sigma_1 \exp\left(\frac{-E_a}{KT}\right)$$

where σ_1 is the pre-exponential factor proportional to the grain size; E_a is the activation energy, K the Boltzmann constant, and T the temperature in Kelvin. From this equation and the data given

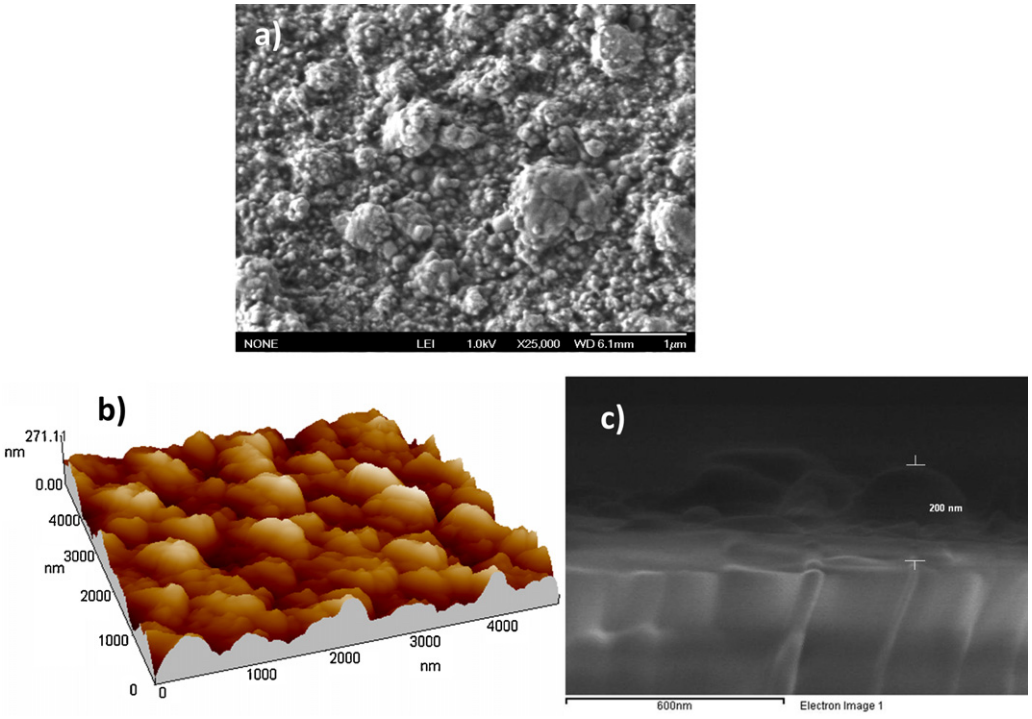

Fig. 2. (a) SEM, (b) AFM, and (c) cross sectional SEM images for $AgInS_2$ film (after annealing the In_2S_3–Ag_2S samples in N_2 at 400 °C for 1 h).

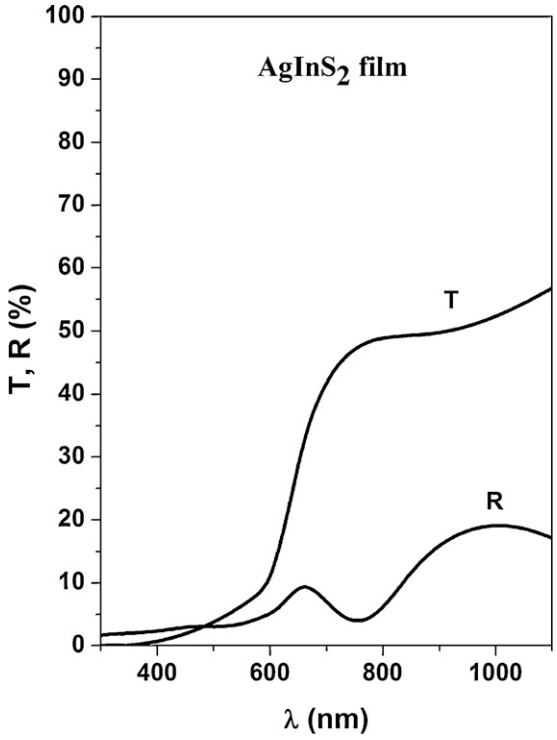

Fig. 3. $T(\lambda)$ and $R(\lambda)$ spectra for $AgInS_2$ films (after annealing the In_2S_3–Ag_2S samples in N_2 at 400 °C for 1 h).

in Fig. 5 we can calculate the activation energy in a given range of temperature. The above equation becomes to:

$$\ln \sigma = \ln \sigma_1 - \frac{E_a}{KT}$$

Calculating the slop in the plot we can determine the activation energy of the film for different ranges of temperature. From

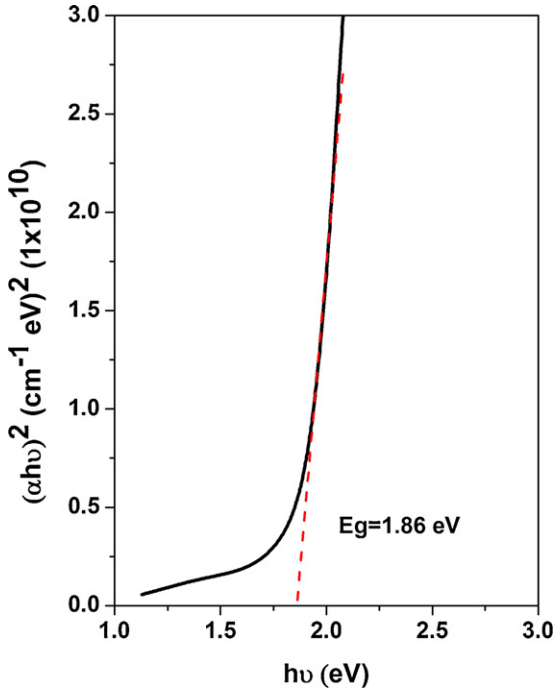

Fig. 4. Plot of $(\alpha h\nu)^2$ vs. $h\nu$ for $AgInS_2$ film (after annealing the In_2S_3–Ag_2S sample in N_2 at 400 °C for 1 h).

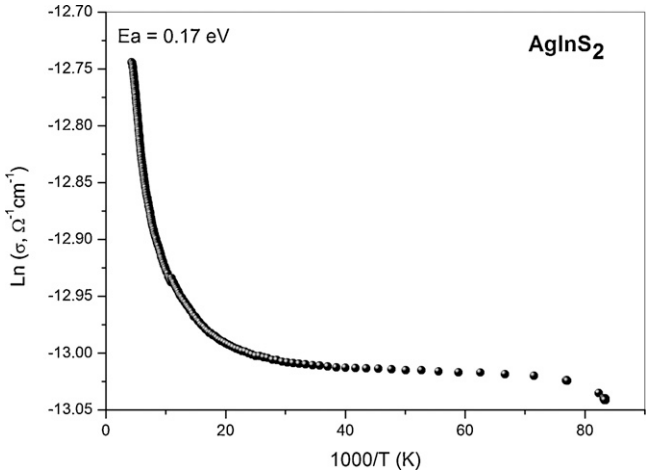

Fig. 5. Temperature dependent conductivity plot for $AgInS_2$ film (after annealing the In_2S_3–Ag_2S sample in N_2 at 400 °C for 1 h).

Fig. 5 we can see that semiconducting behavior of the sample is demonstrated. The activation energy (E_a) was determined for a temperature range of 290–283 K and 166–220 K being 0.17 eV and 5 meV, respectively.

4. Conclusions

We have reported the results of the structural, morphological, optical, and electrical characterizations of $AgInS_2$ thin films obtained by annealing the chemically deposited In_2S_3–Ag_2S layers. According to the XRD and EDX results, heating In_2S_3–Ag_2S layers at 400 °C in N_2 for 1 h, the chalcopyrite structure of $AgInS_2$ can be obtained. This film has an optical band gap, E_g, of 1.86 eV and an electrical conductivity value of $1.2 \times 10^{-3}\,(\Omega\,\mathrm{cm})^{-1}$. The obtained $AgInS_2$ films are suitable for solar cell applications (as a possible buffer layer).

Acknowledgements

This work was supported by PAICYT-UANL 2010 (México) grant of Dra. Y. Peña. Technical assistance of Hugo Salas (Laboratorio de Caracterización Microestructural de Materiales Avanzados-UANL) with FE-SEM measurements, and José Campos (CIE-UNAM) with temperature dependent conductivity measurements, which are strongly appreciated.

References

[1] J.L. Shay, B. Tell, L.M. Schiavone, H.M. Kasper, F. Thiel, Physical Review B 9 (1974) 1719–1723.
[2] J.L. Shay, J.H. Wernick, Ternary Chalcopyrite Semiconductors: Growth, Electronic Properties, and Applications, Pergamon Press, USA, 1975.
[3] R.W. Birkmire, Proc. 26th IEEE PVSC, Anaheim, CA, 1997, p. 295.
[4] K. Okamoto, K. Kinoshita, Solid-State Electronics 19 (1976) 31–35.
[5] K. Yoshino, H. Komaki, T. Kakeno, Y. Akaki, T. Ikari, Journal of Physics and Chemistry of Solids 64 (2003) 1839–1842.
[6] M.L. Albor-Aguilera, D. Ramírez-Rosales, M.A. González-Trujillo, Thin Solid Films 517 (2009) 2535–2537.
[7] Y. Akaki, S. Kurihara, M. Shirahama, K. Tsurugida, T. Kakeno, K. Yoshino, Journal of Materials Science: Materials in Electronics 16 (7) (2005) 393–396.
[8] M. Calixto-Rodriguez, H. Martínez, M.E. Calixto, Y. Peña, D. Martínez-Escobar, A. Tiburcio-Silver, A. Sanchez-Juarez, Materials Science and Engineering B 174 (2010) 253–256.
[9] C.A. Arredondo, J. Clavijo, G. Gordillo, Journal of Physics: Conference Series 167 (2009) 012050.
[10] L. Li-Hau, W. Ching-Chen, L. Chia-Hung, L. Tai-Chou, Chemistry of Materials 20 (2008) 4475–4483.
[11] A. Núñez, M.T.S. Nair, P.K. Nair, Semiconductor Science and Technology 20 (6) (2005) 576–585.

[12] B. Asenjo, A.M. Chaparro, M.T. Gutiérrez, J. Herrero, C. Maffiotte, Electrochimica Acta 49 (2004) 737–744.
[13] W. Vallejo, C. Quiñones, G. Gordillo, Journal of Physics and Chemistry of Solids 72 (2012) 573–578.
[14] Ch. Kong-Wei, H. Chao-Ming, P. Guan-Ting, Ch. Wen-Sheng, L. Tai-Chou, C.K.Y. Thomas, Journal of Photochemistry and Photobiology A: Chemistry 190 (2007) 77–87.
[15] T.S. Moss, Optical Properties of Semiconductors, Butterworths, London, UK, 1959.
[16] K.L. Chopra, S.R. Das, Thin Film Solar Cells, Plenum Press, New York, 1983.
[17] M. Ortega-López, A. Morales-Acevedo, O. Solorza-Feria, Thin Solid Films 385 (2001) 120–125.
[18] R. Caballero, C. Guillén, Thin Solid Films 431-432 (2003) 200–204.